J exp. Biol. 158, 291–306 (1991)
Printed in Great Britain © The Company of Biologists Limited 1991

CIRCULATORY MECHANICS IN THE TOAD *BUFO MARINUS*

II. HAEMODYNAMICS OF THE ARTERIAL WINDKESSEL

BY CAROL A. GIBBONS[1] AND ROBERT E. SHADWICK[2,*]

[1]*Department of Biology, University of Calgary, Calgary, Alberta, Canada T2N 1N4* and [2]*Marine Biology Research Division A-004, Scripps Institution of Oceanography, La Jolla, CA 92093, USA*

Accepted 29 March 1991

Summary

This study examines the importance of vascular elasticity to arterial haemodynamics in a poikilothermic vertebrate. Pulsatile blood pressure, flow and vessel diameter were recorded at several locations within the arterial tree of the toad, *Bufo marinus*. We then determined the dynamic elastic modulus, the pulse wave velocity and the hydraulic impedance characteristics of the aorta. The relatively low heart rate and short arterial tree, and a pulse velocity of about $2.5\,m\,s^{-1}$, combine to give a transit time for the pressure pulse through aorta that is only 3 % of the cardiac cycle. Consequently, wave propagation effects seen in mammals, such as peripheral amplification, distortion and secondary pressure peaks due to reflections, are not apparent. Instead, the aorta acts as a simple Windkessel and inflation by the heart occurs almost simultaneously throughout. Pressure waveforms are nearly identical at proximal and distal locations, and flow pulsatility is reduced progressively through the elastic aorta.

Introduction

The viscoelasticity of the arterial tree is a major haemodynamic determinant that influences the pulse-wave velocity, the hydraulic input impedance and the shape of blood pressure and flow waveforms. Wave propagation effects, such as pulse amplification, distortion and reflections evident as secondary peaks are seen in mammalian circulatory systems, partly because of the 'elastic taper' of the aorta, but primarily as a result of the relatively high heart rates (Taylor, 1964, 1966*b*). These features are not evident in poikilothermic vertebrates or invertebrates that have substantially lower heart rates than comparable-sized mammals (Shelton and Jones, 1965, 1968; Shelton, 1970; Burggren, 1977*b*; Langille and Jones, 1977; West and Burggren, 1984; Shadwick *et al.* 1987). Thus, the mammalian aorta is appropriately modelled as a wave-transmission system (McDonald,

* To whom reprint requests should be sent.

Key words: haemodynamics, arterial elasticity, Windkessel, vascular impedance, pressure wave velocity, *Bufo marinus*.

1974), while the arterial tree of a poikilotherm can be described as a simple Windkessel.

Briefly, the Windkessel model treats the aorta and major arteries as a single compliant chamber linked in series with a single peripheral resistor. Pulse waves are transmitted instantaneously, such that the whole system is inflated in synchrony and no propagation effects occur. Flow into the Windkessel is pulsatile, but the outflow through the peripheral resistor is relatively steady because the pulse is smoothed by the expansion and recoil of the elastic chamber. These conditions hold true for an arterial system where the transit time of the pressure wave is a negligible portion of the time of one cardiac cycle. In mammals this is not the case but in poikilotherms, such as small reptiles and amphibians (Shelton and Jones, 1968; Jones and Shelton 1972; Langille and Jones, 1977; Burggren 1977*a*,*b*; Gibbons and Shadwick, 1989), the heart rate is low and the arterial tree is relatively short compared to the pressure wavelengths. Wave propagation effects are insignificant and, thus, the Windkessel model provides an adequate description of the arterial haemodynamics.

Absent from the literature on cardiovascular mechanics of lower vertebrates are any *in vivo* measurements of arterial elastic properties. In the previous paper (Gibbons and Shadwick, 1991) we showed by *in vitro* mechanical tests that the aorta of the toad is a resilient elastic vessel that has the same functional properties as the aorta in mammals, i.e. at their respective blood pressures these aortas have similar elastic moduli. In the current study we have determined the dynamic elastic modulus of the aorta from *in vivo* measurements of pressure and diameter and predicted the wave velocity and characteristic impedance. In addition, we demonstrate the Windkessel characteristics of the system by an analysis of pressure and flow waveforms obtained at different locations within the arterial tree.

Materials and methods

Experiments were carried out on nine healthy toads (*Bufo marinus* L.) weighing between 300 and 450 g. The animals were anaesthetized by intraperitoneal injection of MS-222 (Sandoz, 1:1000, 0.01 ml g^{-1} body mass). The level of anaesthesia was maintained so that the animal was continually unconscious but breathing regularly. All experiments were acute and terminal, the animals being killed by an excess of MS-222.

Aortic pressure was measured from a cannula inserted dorsally into the subclavian artery up to its junction with the aortic arch. Simultaneously, pressure was measured from a catheter inserted dorsally into the sciatic artery of the leg. Both catheters were less than 15 cm in length. Pressures were measured by two matched Gould P23Db transducers. These were calibrated both dynamically, by the 'pop test' technique (Milnor, 1982), and statically, against a water column. Wave velocity was determined from the time delay between the two pressure signals. The positions of the pressure transducers were then reversed to see if any

phase errors were present. Following this, a mid-line ventral incision was made to expose the aortic arches and dorsal aorta.

Flow was measured by a pulsed Doppler flowmeter (model 545C-4, University of Iowa Bioengineering). The flow probe consisted of a piezoelectric crystal mounted in epoxy resin on a fabric backing which, when placed against the vessel wall, held the crystal face at 45° to the direction of blood flow (for a description of such an instrument, see Milnor, 1982). The range was set to give the maximum signal, indicating that the probe was recording from the midstream of the flow. This instrument has a fixed output of 0.5 volts per kilohertz of frequency shift. From this, a calibration equation can be derived: $Q(\mathrm{l\,min^{-1}})=(XD^2)/(271.2\cos A)$, where Q is flow, X is the voltage of the flow signal, D is the vessel diameter and A is the angle between the crystal face and the vessel long axis (45°). Flow measurements were taken sequentially at the five sites indicated in Fig. 1. At site 5, pressure and flow were measured in contralateral vessels.

Pulsatile changes in aortic diameter were also measured on several animals, using a video dimension analyzer (VDA, Instrumentation for Physiology and Medicine, model 303) as described by Fung (1981). The VDA has a 15 Hz low-pass filter that introduces significant phase shift and attenuation. The frequency response of the VDA was quantified from 0.05 to 15 Hz, using a vibrator and a

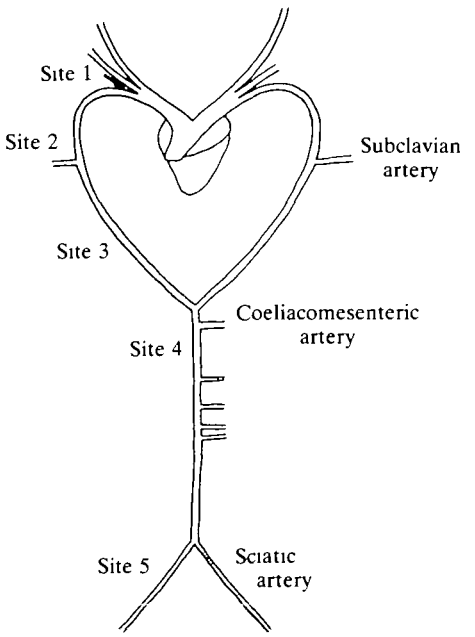

Fig. 1. Diagram of the arterial tree of the toad, *Bufo marinus*, drawn approximately to scale. The five testing sites used are labelled as shown. Site 1 was the most proximal part of the aortic arch. Site 2 was the area just proximal to the subclavian artery. Site 3 was between the subclavian artery and the coeliacomesenteric artery. Site 4 was just distal to the coeliacomesenteric artery. Site 5 was in the sciatic artery. The length of the arterial tree, from the heart to the abdominal bifurcation, was approximately 11 cm.

transfer function analyzer (series SM272, SE Laboratories), as described previously (Shadwick and Gosline, 1985). Appropriate corrections were made to the phase and amplitude for each harmonic component of the diameter waveforms.

Pressure, flow and diameter were recorded on an FM tape recorder. Subsequent analogue-to-digital conversion was performed by a PDP-11/23 laboratory computer (Digital Equipment Corporation) at a sampling rate of $100\,s^{-1}$. Signal-averaged pulses were subjected to Fourier analysis. The amplitude and phase were calculated for nine harmonics. The application of this technique to haemodynamics is described by McDonald (1974) and Milnor (1982).

The mean peripheral resistance, $\boldsymbol{R}$, can be calculated from the mean pressure (P_0) and the mean flow (Q_0) as $\boldsymbol{R}=P_0/Q_0$. The input impedance is a dynamic analogue of peripheral resistance. Therefore, impedance amplitude (Z) is calculated for each harmonic frequency as $Z_n=P_n/Q_n$, where P_n and Q_n are the respective amplitudes of the nth harmonics of pressure and flow waves. The phase (ϕ) is calculated from $\phi_n=\beta_n-\alpha_n$, where α_n and β_n are, respectively, the phase shifts of the nth harmonic of pressure and flow.

The input impedance is equivalent to the characteristic impedance, Z_c, if no reflected waves are present (McDonald, 1974). This can be calculated from the physical properties of the vessel, neglecting viscosity, as:

$$Z_c = \rho c/\pi r^2, \tag{1}$$

where c is the characteristic pressure wave velocity (see equation 4), r is the internal radius and ρ is the blood density. Impedance calculations for a Windkessel model were made using an electrical analogue, as described by Langille and Jones (1977). This involves determining τ, the time constant of diastolic pressure decay, from the pressure pulse profile as:

$$\tau = t/\ln(P_i/P_d) = \boldsymbol{RC}, \tag{2}$$

where t is the duration of diastole, P_i is the pressure at the onset of diastole, P_d is the pressure at the end of diastole and C is the compliance of the elastic aorta.

The dynamic elastic modulus of the aorta (E_{dyn}) was determined at physiological pressures from the pressure and radius harmonics:

$$E_{dyn} = 0.75(R^2/h)(P_n/R_n), \tag{3}$$

where R is the mid-wall radius, h is the wall thickness and P_n and R_n are the harmonic amplitudes of pressure and radius, respectively, obtained by Fourier analysis. This relationship is derived from Bergel (1961), with the assumption that the artery is a thin-walled tube. The characteristic wave velocity (c) can be calculated as:

$$c = (E_{dyn}h/2R\rho)^{0.5}. \tag{4}$$

The apparent pressure wave velocity (c') was calculated by comparing the phase differences of the fundamental harmonics of the proximal and distal pressure waveforms. Dynamic pressure–diameter relationships were also recorded from a

cannulated aorta *in vitro* by introducing a sinusoidal pulse through a syringe attached to a vibrator. The vibrator was driven at frequencies varying from 0.5 to 7 Hz. The mean pressure of the system was set by a static pressure head. Measurements were taken at mean pressures of 1.2, 1.8, 2.6 and 3.6 kPa. The phase and amplitude of the pressure and diameter waves were determined using the transfer function analyzer. Dynamic elastic modulus was then calculated for each test frequency using equation 3 and compared with those values obtained from *in vivo* measurements.

Results

Pressure and flow relationships

Fig. 2 shows examples of blood pressure waves recorded simultaneously at the aortic arch and 11 cm distally at the top of the sciatic artery. These waveforms are typical of those recorded previously in this species and from other poikilotherms (Shelton and Jones, 1968; Shelton and Burggren, 1976; Langille and Jones, 1977; Burggren, 1977*b*; West and Burggren, 1984; Shadwick *et al.* 1987). Pressure falls smoothly during diastole and no secondary peaks are evident. The onset of diastole is not marked by an incisura but only by an inflection in the slope of the descending wave. There is essentially no change in the shape of the pressure wave between the aortic arch and the sciatic artery, and only a small degree of attenuation.

The mean arterial pressure generally ranged from 2.5 to 3 kPa and the pulse pressure ranged from 1.7 to 2.0 kPa. These are similar to values obtained in previous studies on anaesthetized toads (Shelton and Jones, 1968; Kirby and Burnstock, 1969) but lower than those recorded in pithed toads by Van Vliet and West (1987*a*,*b*). In the latter studies, blood pressures of 4.5–6.5 kPa were

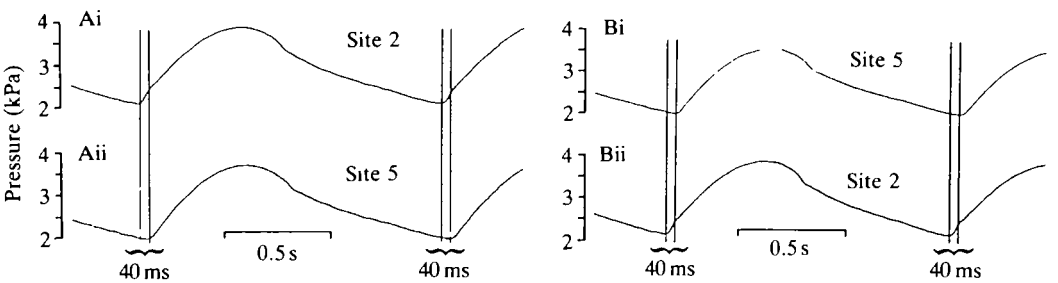

Fig. 2. Simultaneous recordings of pressure at two of the sites defined in Fig. 1. (A) The subclavian pressure recorded through transducer 1 (Ai), and the sciatic pressure recorded through transducer 2 (Aii). (B) The cannulae leading into the transducers are switched. The subclavian pressure is now recorded through transducer 2 (Bii), while the sciatic pressure is recorded through transducer 1 (Bi). In both cases there was a 40 ms delay between the pulse seen in the subclavian artery (Ai, Bii) and the pulse seen in the sciatic artery (Aii, Bi), indicating that the delay is due to the transit time of the pulse and not to the response characteristics of the two transducers.

reported, while in conscious and anaesthetized toads aortic pressures range from 3 to 4.5 kPa (Van Vliet and West, 1986; West and Burrgren, 1984).

Pressure pulses from the aortic arch and the sciatic artery were separated by 40–45 ms, as measured by the position of the wave front (Fig. 2). When the catheters were interchanged to feed into the opposite transducers, the time delay remained, indicating that no phase errors were introduced by the transducers.

The pulse velocity calculated from the time delay of the distal pressure wave was 2.4–2.75 m s^{-1}. Heart rate averaged 37 min^{-1} (0.62 Hz), giving a wavelength for the fundamental frequency of about 4.2 m. Fourier analysis of signal-averaged waveforms showed a phase shift of 9–11° in the fundamental harmonics. This yields a pressure wave velocity of 2.25–2.75 m s^{-1} (see Table 1).

Fig. 3 shows examples of blood flow pulses recorded at different levels in the arterial tree of one toad. Peak flows in all our specimens ranged from 0.5 to 0.9 ml s^{-1} in the aortic arch (site 1), from 0.45 to 0.75 ml s^{-1} in the dorsal aorta (site 4) and from 0.2 to 0.35 ml s^{-1} in the sciatic artery (site 5). The end of systole is marked by a slight flow reversal in recordings from the top of the aortic arch only (Fig. 3), presumably indicating closure of the ventricular valves (Shelton, 1970; Langille and Jones, 1977). The positive diastolic flow immediately following this reversal may result from contraction of the conus arteriosus (Langille and Jones,

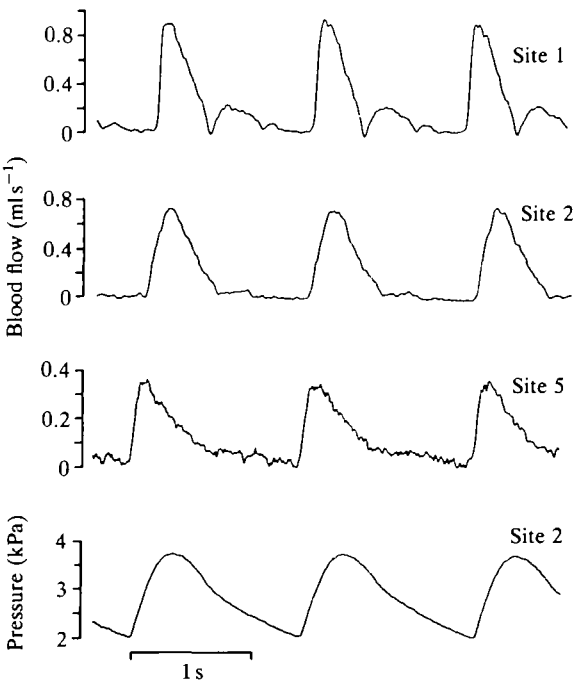

Fig. 3. Flow at three of the sites along the length of the aorta shown in Fig. 1. These recordings were not made simultaneously, but were correlated in each case with a simultaneous pressure recording. With increased distance from the heart, pulsatility decreases, flow reversal disappears and the diastolic flow remains positive.

1977), but this was not always observed in our experiments. Negative flow does not occur at the other arterial locations (Fig. 3). In the lower portion of the aortic arch (site 2) the flow drops rapidly in diastole and remains near zero for over half of the diastolic period. In contrast, flow in the sciatic artery decreases more gradually during diastole, not reaching zero until just before the beginning of the next cycle. These changes demonstrate that the blood flow pulse is being smoothed as it travels through the elastic aorta. In contrast, negative flow and secondary peaks in pressure and flow occur in the mammalian system at sites as peripheral as the femoral artery (McDonald, 1974), owing to the interaction of reflected waves. Blood flow in the distal part of the toad aorta is never negative and falls to zero only at the end of each pulse (Fig. 3)

Fig. 4 shows trains of pressure and flow pulses in the lower aortic arch (site 2) that have been digitized, signal-averaged and subjected to Fourier analysis. The amplitudes of the first nine harmonics of pressure and flow are shown in Fig. 5. The mean pressure and flow are the zero harmonics. Heart rate determines the frequency of the first harmonic, and higher harmonics are multiples of this fundamental frequency. The relatively small amplitude of harmonics above the third results from the smooth shapes of pressure and flow waveforms and the absence of any secondary peaks. In this example, 97 % of the pulsatile hydraulic power (see Milnor, 1982) is represented by the first three harmonic pairs.

Vascular impedance spectra for three animals are shown in Fig. 6. Impedance amplitude was normalized to $\boldsymbol{R}$ (the zero frequency value) to account for slight differences in animal size. This ratio falls sharply with the first harmonic and remains relatively constant up to 5 Hz. The final values are less than 10 % of the peripheral resistance but remain above the characteristic impedance Z_c. Impedance phase was negative at all frequencies, indicating that flow peaks ahead of

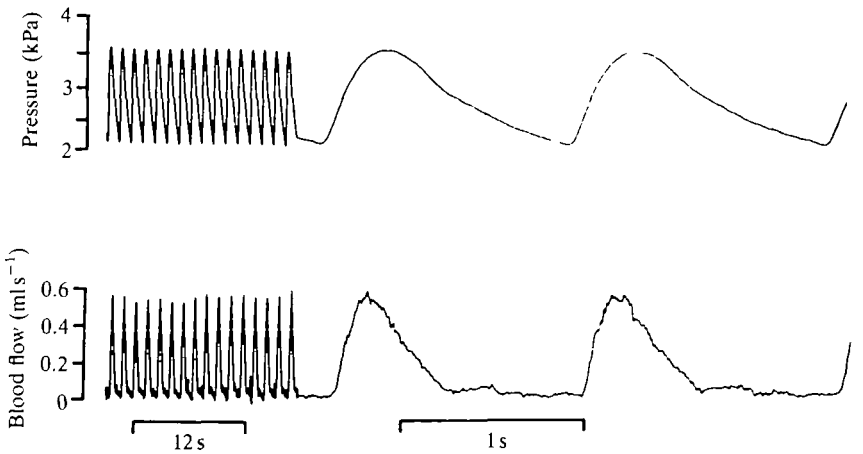

Fig. 4. Examples of simultaneous pressure and flow recordings from site 2 in a different animal from that shown in Fig. 3. Ten of these consecutive pulses were signal-averaged and then digitized for impedance calculations.

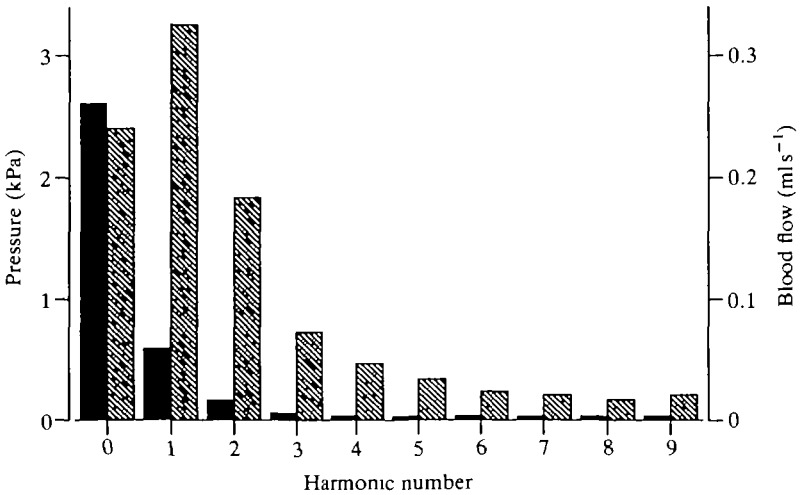

Fig. 5. The amplitudes of the first nine harmonics of pressure (solid bars) and flow (hatched bars) from the waveforms shown in Fig. 4, calculated from Fourier analysis. The zero harmonic is the mean value and the first harmonic occurs at the fundamental frequency of 0.6 Hz in this case.

pressure by about 80° on average. This is close to the limiting value of 90° expected in a Windkessel model (see Fig. 8; Milnor, 1982).

Fig. 7 shows impedance curves for sites 2–5 in the arterial tree of one animal. Since pressures were not recorded at sites 3 and 4, the pressure pulse measured simultaneously at site 2 was substituted for these impedance calculations. This required a slight phase shift in the pressure pulse so that its wave front coincided with that of the flow pulse. With progression towards the periphery the impedance curves are shifted upwards and to the right because the flow becomes less pulsatile and smaller, but the pressure does not.

Fig. 8 shows the close agreement between impedance data from one animal and a curve for the Windkessel model, calculated from the aortic time constant according to equation 2.

Dynamic elastic properties

Fig. 9 shows an example of pressure and diameter pulses recorded simultaneously at site 4. The shapes of the pressure and diameter waves are very similar because the radial displacement of the artery wall is correlated with pressure changes rather than flow. Peak aortic diameter at this location ranged from 2.0 to 2.3 mm, with diastolic values from 1.8 to 2.1 mm at mean blood pressure of 2.9 kPa. Recordings were also made at pressure levels that occasionally ranged as high as 4.0 kPa and as low as 1.3 kPa. In Fig. 10 the dynamic elastic modulus is plotted as a function of frequency at several mean pressures. The curves derived from *in vivo* pulses and those calculated from forced sinusoidal oscillations *in vitro* show similar trends, i.e. E_{dyn} increases with pressure, but is relatively insensitive

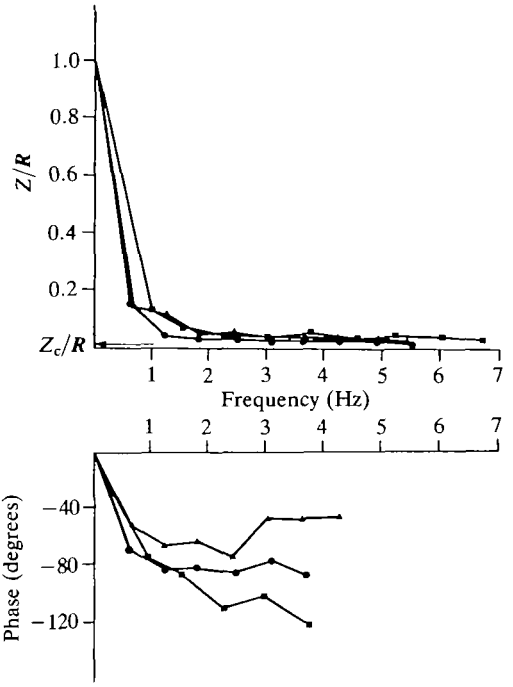

Fig. 6. Normalized impedance spectra for three different toads. The data represent the signal-averaged pulses of pressure and flow. The peripheral resistance, $\boldsymbol{R}$, is taken as the impedance amplitude at the zero-frequency harmonic (i.e. P_0/Q_0). The normalized impedance values are divided by $\boldsymbol{R}$ in each case. The $\boldsymbol{R}$ values for these toads were 10.8, 11.7 and 8.8 kPa s ml^{-1}. Characteristic impedance, Z_c, is also represented as a proportion of $\boldsymbol{R}$. Negative phase values indicate that flow leads pressure.

to increasing frequency. Results from the *in vivo* and *in vitro* tests are in close agreement up to about 2 kPa, but diverge somewhat at higher pressures. These differences probably arise from the different methodologies employed in the two types of test, and we believe that the results in Fig. 10 support the premise that the mechanical properties of the isolated aortic segment are essentially the same as those of the intact aorta *in vivo*. Phase differences between pressure and diameter harmonics (after correction for the VDA response) were typically from 5 to 15°, but showed no apparent frequency or pressure dependence. Values of c, calculated from both *in vivo* and *in vitro* determinations of E_{dyn}, ranged from 2.08 to 2.46 m s^{-1} and from 2.23 to 2.95 m s^{-1}, respectively (Table 1).

Discussion

This study demonstrates the direct effects of aortic elasticity on haemodynamic relationships in the arterial system of a typical poikilothermic vertebrate. The size and shape of the pressure pulse, the pressure wave velocity, the smoothing of the

flow pulse as it travels distally and the hydraulic impedance of the arterial tree are all strongly influenced by the dynamic elastic modulus of the arterial wall. The combination of these elasticity-based properties with the relatively low heart rate and short arterial length results in wave transmission characteristics that are quite different from those of the mammalian circulation and, consequently, can be described by the simple Windkessel model. Thus, the aorta acts essentially as a

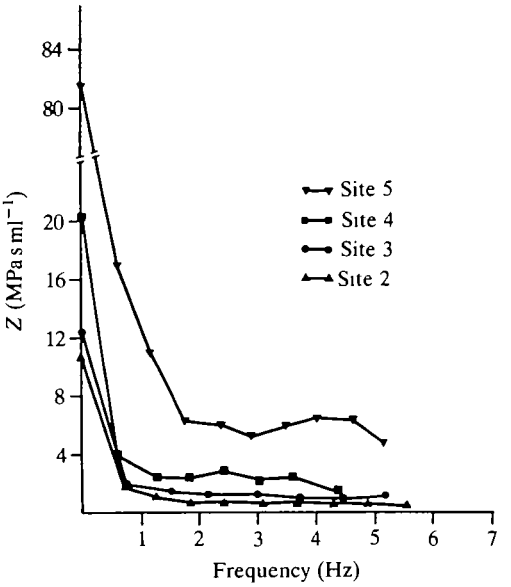

Fig. 7. Impedance values for a single animal calculated from pressure and flow waveforms recorded at four sites along the aortic length. With increasing distance from the heart the impedance values at each frequency increase. Phase values (not shown) were all negative, indicating that flow precedes pressure.

Table 1. *Pressure wave velocities at mean pressures of 2.5–3 kPa, determined by four different methods*

	Dynamic elastic modulus		Simultaneous pressure pulses	
Method	*In vivo*	*In vitro*	Phase shift	Time delay
c or c' ($m\,s^{-1}$)	2.08–2.46	2.23–2.95	2.25–2.75	2.40–2.75

Values are the ranges from six animals.

The velocities calculated from the dynamic elastic modulus (both *in vivo* and *in vitro*) were obtained using equation 4.

The *in vivo* phase shift given in the fourth column was obtained by Fourier analysis of two pressure waves 11 cm apart.

The time delay given in the fifth column was measured from pressure wave fronts at two sites 11 cm apart.

c, characteristic wave velocity; c', apparent pressure wave velocity.

single capacitance element with uniform elastic properties, and inflation by the heart occurs almost simultaneously throughout. In general, these characteristics should be found in any circulatory system where the transit time of the pressure pulse through the arterial tree is a negligible fraction of the cardiac cycle (Langille and Jones, 1977). In this regard, the critical haemodynamic parameters are the pressure-wave velocity, the length of the arterial tree and the frequency of the heartbeat.

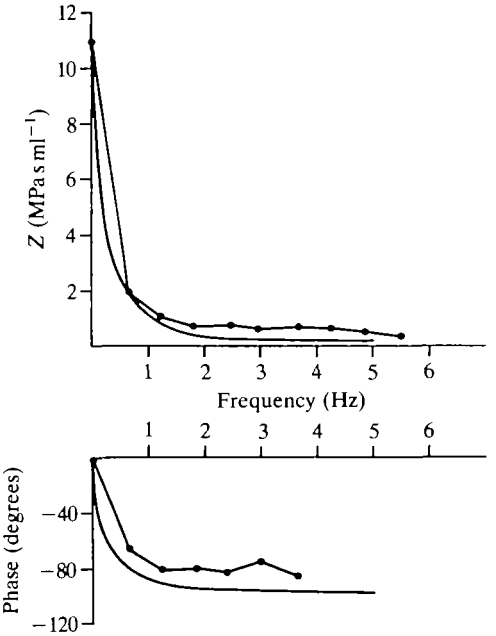

Fig. 8. A comparison of an impedance spectrum obtained experimentally with that calculated from the Windkessel model for the pressure and flow waveforms in Fig. 4. τ, the time constant of diastolic pressure decay, was 1.845 s and $\boldsymbol{R}$, the mean peripheral resistance, was 10.8 kPa s ml^{-1}.

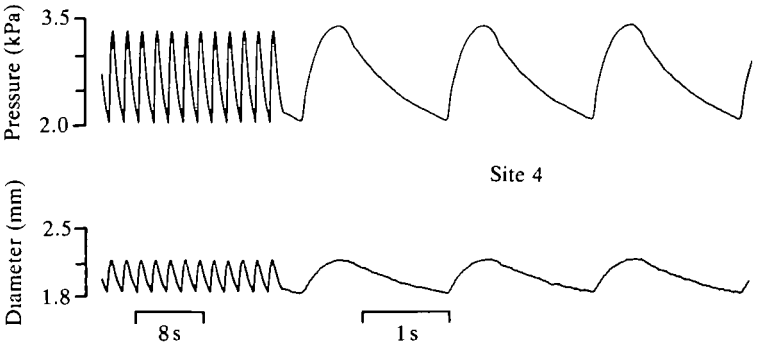

Fig. 9. Simultaneous arterial pressure and diameter recordings from a single animal. Pressure and diameter were taken at four sites, and this figure shows a typical recording from the dorsal aorta (site 4).

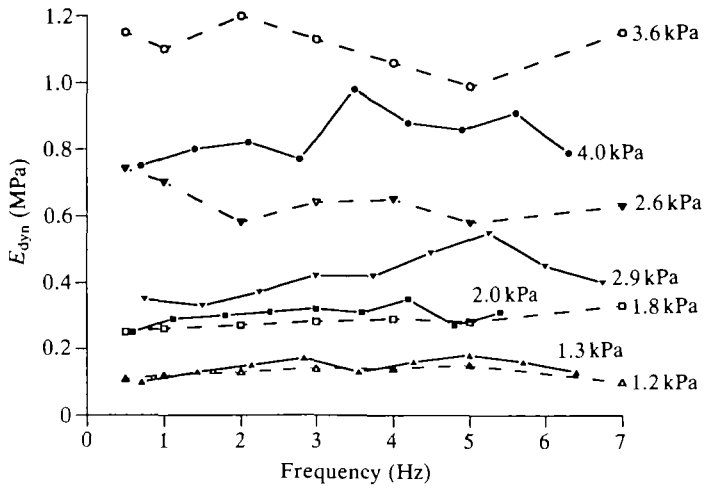

Fig. 10. Dynamic elastic modulus (E_{dyn}) *versus* frequency for different mean pressures. Values were obtained either by Fourier analysis of pressure and diameter waveforms (solid lines) *in vivo* or from sinusoidal inflation of a vessel segment *in vitro* (broken lines).

Pressure-wave velocity can be calculated from the physical properties of the vessel and the fluid in it (equation 4), but it is often determined empirically from the time difference between proximal and distal pressure waves *in vivo* (McDonald, 1974). We compared these methods and found that the values of c calculated from *in vivo* and *in vitro* measurements of E_{dyn} were very similar to the values of c' determined from proximal and distal pressure pulses (Table 1). This is an important result because it demonstrates that the properties of isolated segments measured *in vitro* do represent the *in vivo* elastic behaviour of the aorta and, furthermore, that the elasticity of the vessel wall indeed determines the wave velocity, according to the theoretical relationship of equation 1. Our measurements of E_{dyn} from *in vivo* pressure and diameter pulses are the only ones reported for any non-mammalian vertebrate. Arterial pressure wave velocities in the range of 2–3 $m\,s^{-1}$ (Table 1) are also typical of other poikilothermic vertebrates (Shelton and Jones, 1968; Langille and Jones, 1977; Gibbons and Shadwick, 1989), but somewhat lower than that observed in the mammalian aorta, particularly at its more distal portions. The pulse velocity for mammalian species ranges from 4.10 to 4.70 $m\,s^{-1}$ in the thoracic aorta and increases distally due to the 'elastic taper' that is characteristic of the mammalian aorta (Taylor, 1973; Avolio *et al.* 1976; Cox, 1975).

The average length of the arterial tree, from the aortic arch to the sciatic artery, was 11 cm in a 350 g toad. Assuming that the major reflection site is the abdominal bifurcation, the transit time of a pulse through the aorta would be only 0.05 s, or approximately 3 % of the cardiac cycle (Table 2). This means there is time for up to 30 reflections of a pulse within one heartbeat period. The pressure amplitud

Table 2. *Haemodynamic parameters of characteristic wave velocity* c_0, *fundamental frequency* f_0, *and fundamental wavelength* λ

Animal	c ($m\,s^{-1}$)	f_0 (Hz)	λ (m)	L/λ	Transit time (s)	Percentage of cardiac cycle
1	2.09	0.7	2.98	0.04	0.05	3.5
2	2.57	0.69	3.74	0.03	0.04	2.8
3	2.37	0.65	3.65	0.03	0.05	3.3

Values are means for three toads.

Pulse transit time is given in seconds and as a percentage of the cardiac cycle. c, the characteristic wave velocity, is calculated from equation 4 and λ is calculated from $c=f_0\lambda$.

The fundamental frequency, f_0, is equivalent to the heart rate.

The length of the arterial tree (L) averaged 11 cm in these animals.

will diminish rapidly as the wave travels because energy is lost to blood and artery wall viscosity, and because the reflection is incomplete, such that each wave is essentially attenuated before the next begins. Therefore, wave reflections from one pulse do not significantly affect the size or shape of any successive pulses, and wave transmission effects such as peripheral amplification, distortion or secondary peaks in diastole are not evident (Fig. 2). This results in the pressure waveforms at proximal and distal sites being nearly identical. This conclusion is in agreement with those of previous haemodynamic studies on other poikilothermic vertebrates (Shelton and Jones, 1968; Shelton, 1970; Shelton and Burggren, 1976; Burggren 1977*a*; Langille and Jones, 1977; Avolio *et al.* 1983; Gibbons and Shadwick, 1989) and invertebrates (Shadwick *et al.* 1987, 1990). It is interesting to note that viscous damping in the aorta (due to wall and blood viscosity), reduces the elastic efficiency of the system, but is an important feature of the Windkessel because it helps attenuate the reflected pressure waves, thus preventing resonance from occurring.

The lack of wave propagation effects in a Windkessel results in an impedance spectrum that is a continuously decreasing function of frequency (Fig. 8), where Z remains above Z_c at the fundamental heart frequency (Fig. 6). In contrast, a transmission-line system generates oscillations in Z above and below Z_c, with the first minimum coming at a frequency where the distance to the major reflecting site (L) is one-quarter of the wavelength (λ) (Fig. 11). This occurs in mammals at about the fundamental frequency (Milnor, 1982), but in poikilotherms the L/λ ratio at the fundamental frequency is very much less than 0.25 (Table 2; Gibbons and Shadwick, 1989), primarily because of their comparatively low heart rates. In the toad, for example, the quarter-wavelength frequency would occur at about 6 Hz, or the eighth harmonic, and this represents an insignificant component of the pressure pulse (Fig. 5). In comparison, the quarter-wavelength frequency for a 350 g rat would occur at about 7 Hz, which is nearly its resting heart rate. Although specific differences exist between the physical properties of the aorta in the

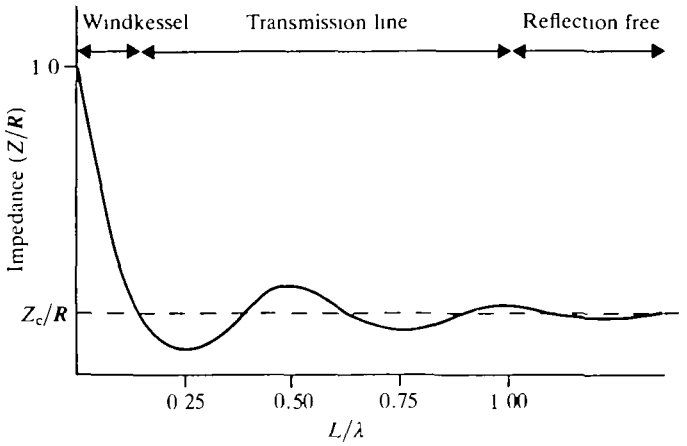

Fig. 11. A generalized curve showing impedance amplitude as a function of frequency expressed as the ratio of the arterial tree length (L) to the fundamental pressure wavelength (λ). A short arterial tree and/or a low heart rate shift the impedance spectrum to the left, making the system function as a Windkessel. A very long arterial tree or a very high heart rate shifts the spectrum to the right, making it more like a reflection-free transmission line.

toad and mammals, namely the presence of a geometric and elastic taper in the latter (Gibbons and Shadwick, 1991), these alone do not determine whether their arterial systems function as Windkessels or transmission lines. The most important haemodymanic difference between the toad and similar-sized mammals that influences L/λ, and thus determines whether the aorta acts as a Windkessel or a transmission line, is the heart rate.

Taylor (1964) proposed that the elastic taper of the mammalian aorta acts like a series of wave reflection sites distributed along the length of the vessel. The effect of this feature in a transmission line system is to amplify incident waves, attenuate reflected waves and increase the impedance oscillations which, in turn, reduce the work of the heart (Taylor, 1965, 1966*a*,*b*; O'Rourke and Taylor, 1967). In the toad circulation, where transmission effects do not dominate, an elastic taper of the aorta would appear to be unnecessary, and does not occur (Gibbons and Shadwick, 1991).

In addition to being the major blood conduit from the ventricle, the aorta in poikilotherms, like the toad, and in mammals is designed to provide a major pulse-smoothing effect. Specific differences in the structure and connective tissue composition of the artery wall have evolved to suit each to the particular pressure range encountered. Major differences in the haemodynamic properties in these two groups arise not because of functionally different aortic elastic properties but primarily because of very different heart rates.

This work was supported by a Graduate Research Grant from the University of Calgary to C.A.G. and by an operating grant and Research Fellowship from the Natural Science and Engineering Research Council of Canada to R.E.S.

References

AVOLIO, A. P., O'ROURKE, M. F., MANG, K., BASON, P. T. AND GOW, B. S. (1976). A comparative study of pulsatile arterial haemodynamics in rabbits and guinea pigs. *Am. J. Physiol.* **230**, 868–875.

AVOLIO, A. P., O'ROURKE, M. F. AND WEBSTER, M. E. D. (1983). Pulse-wave propagation in the arterial system of the diamond python, *Morelia spilotes*. *Am. J. Physiol.* **246**, R267–R270.

BERGEL, D. H. (1961). The dynamic elastic properties of the arterial wall. *J. Physiol., Lond.* **156**, 458–469.

BURGGREN, W. W. (1977*a*). The pulmonary circulation of the chelonian reptile: morphology, haemodynamics, and pharmacology. *J. comp. Physiol.* B **116**, 303–323.

BURGGREN, W. W. (1977*b*). Circulation during intermittent lung ventilation in the garter snake, *Thamnophis*. *Can. J. Zool.* **55**, 1720–1725.

COX, R. H. (1975). Pressure dependence of the mechanical properties of arteries *in vivo*. *Am. J. Physiol.* **36**, 1371–1375.

FUNG, Y. C. (1981). *Biomechanics – Mechanical Properties of Living Tissues*. New York: Springer-Verlag.

GIBBONS, C. A. AND SHADWICK, R. E. (1989). Mechanical design in the arteries of lower vertebrates. *Experientia* **45**, 1083–1088.

GIBBONS, C. A. AND SHADWICK, R. E. (1991). Circulatory mechanics in the toad *Bufo marinus*. I. Structure and mechanical design of the aorta. *J. exp. Biol.* **158**, 275–289.

JONES, D. R. AND SHELTON, G. (1972). Factors affecting diastolic blood pressures in the systemic and pulmocutaneous arches of anuran amphibia. *J. exp. Biol.* **57**, 789–803.

KIRBY, S. E. AND BURNSTOCK, G. (1969). Pharmacological studies of the cardiovascular system in the anaesthetized sleepy lizard (*Tiliqua rugosa*) and the toad (*Bufo marinus*). *Comp. Biochem. Physiol.* **28**, 321–331.

LANGILLE, B. L. AND JONES, D. R. (1977). Dynamics of blood flow through the heart and arterial systems of anuran amphibia. *J. exp. Biol.* **68**, 1–17.

MCDONALD, D. A. (1974). *Blood Flow in Arteries*. London: Edward Arnold.

MILNOR, W. R. (1982). *Hemodynamics*. Baltimore: Williams and Wilkens.

O'ROURKE, M. F. AND TAYLOR, M. G. (1967). Input impedance of the systemic circulation. *Circulation Res.* **20**, 365–372.

SHADWICK, R. E. AND GOSLINE, J. M. (1985). Mechanical properties of the octopus aorta. *J. exp. Biol.* **114**, 259–284.

SHADWICK, R. E., GOSLINE, J. M. AND MILSOM, W. K. (1987). Arterial haemodynamics in the cephalopod mollusc, *Octopus dofleini*. *J. exp. Biol.* **130**, 87–106.

SHADWICK, R. E., POLLOCK, C. M. AND STRICKER, S. A. (1990). Structure and biomechanical properties of crustacean blood vessels. *Physiol. Zool.* **63**, 90–101.

SHELTON, G. (1970). The effect of lung ventilation on blood flow to the lungs and body of the amphibian, *Xenopus laevis*. *Respir. Physiol.* **9**, 183–196.

SHELTON, G. AND BURGGREN, W. W. (1976). Cardiovascular dynamics of the chelonia during apnoea and lung ventilation. *J. exp. Biol.* **64**, 323–343.

SHELTON, G. AND JONES, D. R. (1965). Central blood pressure and heart output in surfaced and submerged frogs. *J. exp. Biol.* **42**, 339–357.

SHELTON, G. AND JONES, D. R. (1968). A comparative study of central blood pressures in five amphibians. *J. exp. Biol.* **49**, 631–643.

TAYLOR, M. G. (1964). Wave travel in arteries and the design of the cardiovascular system. In *Pulsatile Blood Flow* (ed. E. O. Attinger), pp. 343–372. New York: McGraw-Hill.

TAYLOR, M. G. (1965). Wave travel in a non-uniform transmission line in relation to pulses in arteries. *Phys. med. Biol.* **10**, 539–550.

TAYLOR, M. G. (1966*a*). The input impedance of an assembly of randomly branching elastic tubes. *Biophys. J.* **6**, 29–51.

TAYLOR, M. G. (1966*b*). Wave transmission through an assembly of randomly branching elastic tubes. *Biophys. J.* **6**, 697–716.

TAYLOR, M. G. (1973). Hemodynamics. *A. Rev. Physiol.* **35**, 87–116.

VAN VLIET, B. N. AND WEST, N. H. (1986). Cardiovascular responses to electrical stimulation of

the recurrent laryngeal nerve in conscious toads (*Bufo marinus*). *J. comp. Physiol.* B **156**, 363–375.

VAN VLIET, B. N. AND WEST, N. H. (1987*a*). Responses to circulatory pressures and conduction velocity of pulmocutaneous baroreceptors in *Bufo marinus*. *J. Physiol., Lond.* **388**, 41–53.

VAN VLIET, B. N. AND WEST, N. H. (1987*b*). Response characteristics of pulmocutaneous arterial baroreceptors in the toad, *Bufo marinus*. *J. Physiol., Lond.* **388**, 55–70.

WEST, N. H. AND BURGGREN, W. W. (1984). Factors influencing pulmonary and cutaneous arterial blood flow in the toad, *Bufo marinus*. *Am. J. Physiol.* **247**, R884–R894.